

# Synthesis, Characterization and Biological Activity Studies on Novel 4-Chloro-2-[(1-Phenyl-1H-Tetrazol-5-Ylimino)-Methyl] Phenol and Its Metal Complexes

Ranjithreddy Palreddy, Jaheer Mohmed, Nagula Narsimha, Boinala Aparna, Mariyam, Ch. Sarala Devi\*

Department of Chemistry, University College of Science, Osmania University, Hyderabad, India  
Email: [prof.saraladevi.ch@gmail.com](mailto:prof.saraladevi.ch@gmail.com)

Received 4 September 2015; accepted 27 October 2015; published 30 October 2015

Copyright © 2015 by authors and Scientific Research Publishing Inc.

This work is licensed under the Creative Commons Attribution International License (CC BY).

<http://creativecommons.org/licenses/by/4.0/>



Open Access

## Abstract

Novel 4-Chloro-2-[(1-phenyl-1H-tetrazol-5-ylimino)-methyl] phenol (Cl-PTMP) and its transition metal complexes were synthesized and characterized by FT-IR, <sup>1</sup>H-NMR, UV-Vis spectroscopy, Mass spectrometry, TGA and SEM. The pH-metric technique was applied to get an insight of the number of dissociable protons and protonation sites in candidate compound. The pH-Metric studies were also carried out in presence of metal ions to establish the formation of corresponding metal complexes in solution. Further, the metal ligand compositions of Cu (II) and Co (II) complexes were determined spectrophotometrically by employing Job's continuous variation method. To know the molecular properties in title imine compound suitable for metal ion coordination, the computational studies were carried out by employing HyperChem 7.5 tools. The energies of HOMO and LUMO frontier orbitals and their electron density contour maps were generated with geometry optimized molecule. Biological activity of Cl-PTMP and its metal complexes was investigated by disc diffusion method.

## Keywords

Synthesis, Cu (II) and Co (II) Complexes, pH-Metry, Spectro-Analytical and Biological Studies

## 1. Introduction

Tetrazoloderivatives have attracted interest because of their unique structure and their applications as antihyper-

\*Corresponding author.

tensive, anti-allergic, antibiotic and anticonvulsant agents [1]-[5]. Number of publications and patents on the preparation, properties and applications of tetrazole derivatives is increasing every year rapidly. The tetrazole functionality plays an important role in medicinal chemistry, primarily due to its ability to serve as the bioequivalent (bioisostere) of the carboxylic acid group [6], and also the class of tetrazole compounds have been used both as anticancer and antimicrobial agents. Earlier work from our laboratory on Cu (II) complex of tetrazole imine base 2-((E)-(1-phenyl-1H-tetrazol-5-ylimino) methyl) phenol (PTMP) revealed its antimicrobial and DNA cleavage activity [7]. Keeping in view the various applications of tetrazoles and in continuation of work reported earlier, in the present investigation synthesis of 4-Chloro-2-[(1-phenyl-1H-tetrazol-5-ylimino)-methyl] phenol (Cl-PTMP), characterization, molecular properties and metal ion interaction studies were envisaged. Further solid metal complexes of Cl-PTMP were isolated and screened for anti-bacterial activity.

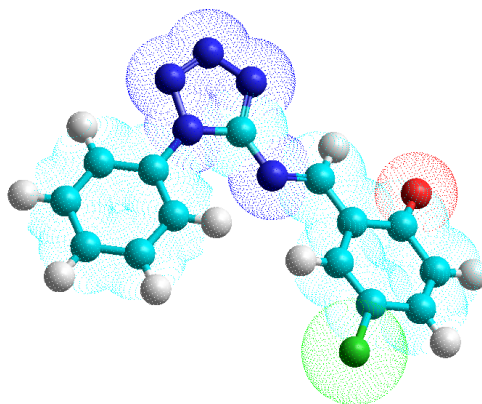
## 2. Experimental

### 2.1. Physical Measurements

All chemicals used are AR grade. UV-Visible spectra were recorded on Shimadzu UV spectrophotometer at 200 - 900 nm wavelength range. The Infrared spectra were recorded on a Perkin-Elmer 337 spectrometer using potassium bromide pellets. <sup>1</sup>H-NMR spectra were recorded on Varian Gemini unity spectrometer and Mass spectra on VG AUTOSPEC. The pH measurements were done using a digital ELICO electronic model LI 120 pH meter in conjugation with a combined glass and calomel electrode. The computational studies were carried out by using Hyperchem 7.5. The surface morphology of the Cl-PTP and its metal complexes was examined using Zeiss SEM (Scanning Electron Microscope) and for the elemental analyses INCA EDX instrument was employed. Melting points were measured on Cintex melting point apparatus. Thermal studies were carried out using Shimadzu TGA-50H in nitrogen atmosphere. Further, thermo gravimetric (TG) and differential thermal analysis (DTA) of metal complexes were carried out on polmon instrument (Model No. MP-90).

#### 2.1.1. Synthesis of 4-Chloro-2-[(1-Phenyl-1H-Tetrazol-5-Ylimino)-Methyl] Phenol (Cl-PTMP)

The synthesis of 4-Chloro-2-[(1-phenyl-1H-tetrazol-5-ylimino)-methyl]-phenol was achieved by the reaction of equimolar ratios (0.01 mol) of 1-phenyl-1H-tetrazole-5-amine and 5-chloro salicylaldehyde. The mixture was dissolved in methanol (10 ml) and was refluxed for 3 - 4 hours at 60°C - 70°C. The progress of the reaction was monitored by TLC. The solid yellow ligand obtained was filtered and washed with methanol. Recrystallization with methanol yielded pure compound (yield = 82%, m.p = 215°C).



Structure of 4-Chloro-2-[(1-phenyl-1H-tetrazol-5-ylimino)-methyl]-phenol.

#### 2.1.2. Synthesis of Metal Complexes

To the methanolic solution of the metal chlorides, (Cu (II) and Co (II)), the solution of Cl-PTMP in chloroform medium was added drop wise. This mixture was reflux for 10 - 12 hours at 50°C - 60°C. The metal complexes obtained were washed with chloroform and methanol (yield: 85% and 90% for Cu (II) and Co (II) complex respectively with m.p. > 300°C for both).

### 3. Results and Discussion

#### 3.1. Characterization of Cl-PTMP

##### 3.1.1. IR Spectrum

The IR spectrum of Cl-PTMP (**Figure 1**) shows characteristic band at  $1605\text{ cm}^{-1}$  which is attributable to C=N stretching vibration of azomethine group. The peak at  $3055\text{ cm}^{-1}$  in the spectrum corresponds to aromatic CH stretching vibration.

##### 3.1.2. $^1\text{H}$ -NMR

The proton NMR spectrum of Cl-PTMP (**Figure 2**) was recorded in  $\text{CDCl}_3$ . It exhibits signal at  $\delta$  11.6 ppm which corresponds to proton of phenolic OH. The signal at  $\delta$  9.5 ppm is assigned to N=CH proton. Signals in the range  $\delta$  6.9 - 7.7 ppm are attributable to aromatic protons.

##### 3.1.3. Mass Spectrum

The mass spectrum of Cl-PTMP (**Figure 3**) displays a peak at  $m/z = 300$ , which is in accordance with the expected quasi ion peak  $(\text{M}+\text{H})^+$ .

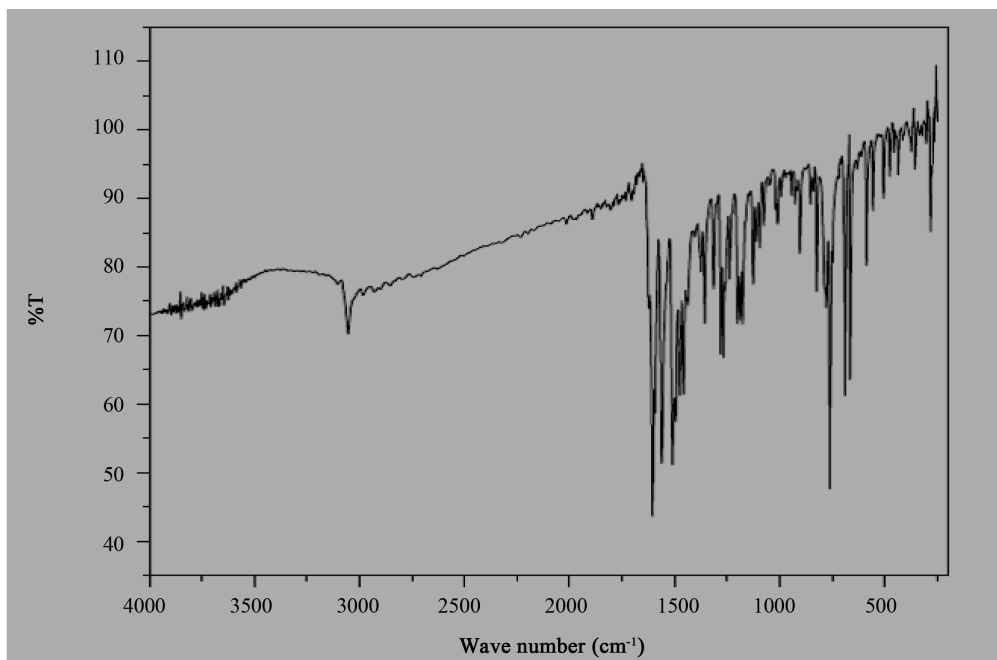


**Figure 1.** IR spectrum of Cl-PTMP.

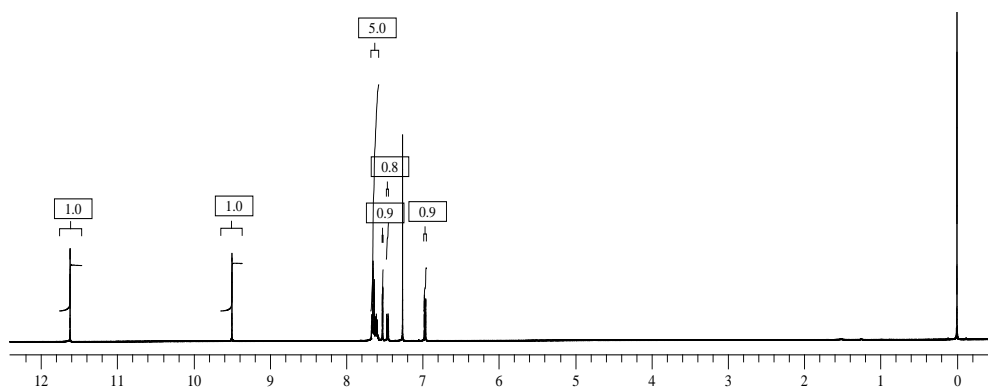


**Figure 2.**  $^1\text{H}$  NMR Spectrum of Cl-PTMP.

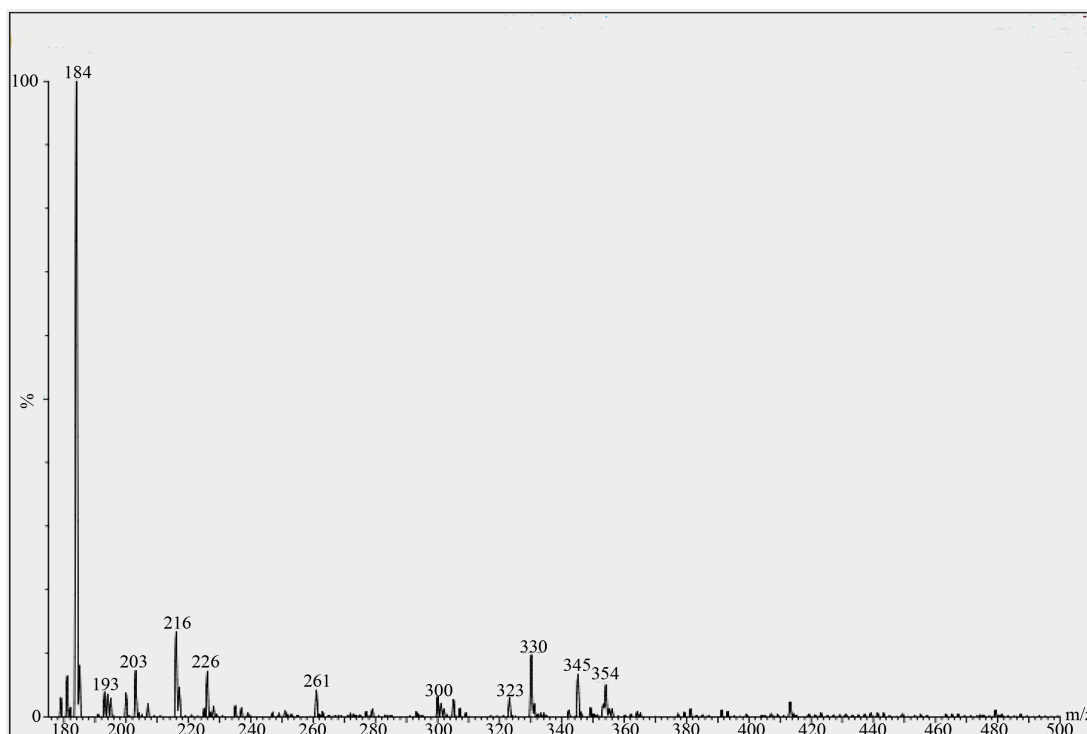


**Figure 3.** Mass spectrum of Cl-PTMP.

### 3.1.4. UV-Visible

The UV spectrum of Cl-PTMP ligand (**Figure 4**) displayed absorption peak at  $34,364.26\text{ cm}^{-1}$  and  $26,315.79\text{ cm}^{-1}$  due to  $\pi - \pi^*$  and  $n - \pi^*$  transitions respectively.

## 3.2. Computational Studies on Cl-PTMP

Quantum chemical calculations have been widely used to study donor and acceptor properties of molecules. The eigen values for molecular orbitals were computed for the geometry optimized molecule of Cl-PTMP using hyperchem 7.5 tools [8]-[12]. As minus eigen values correspond to binding energies of electrons, the computed data is informative to understand electron donating properties of a molecule. The frontier molecular orbital energies (*i.e.*,  $E_{\text{HOMO}}$  and  $E_{\text{LUMO}}$ ) are significant parameters for the prediction of the reactivity of a chemical compound (**Figure 5** and **Figure 6**). The  $E_{\text{HOMO}}$  is often associated with the electron donating ability (Ionization energy) of a molecule. The  $E_{\text{LUMO}}$  indicates the ability of the molecule to accept electrons (Electron affinity). The lower binding energy value  $E_{\text{HOMO}}$  indicates higher tendency for the donation of electrons to the acceptor molecule with suitable low energy and empty molecular orbitals. In the present investigation the values of energy of the highest occupied molecular orbitals ( $E_{\text{HOMO}}$ ) and energy of the lowest unoccupied molecular orbitals ( $E_{\text{LUMO}}$ ) of Cl-PTMP molecule as well as the corresponding orbital contour maps were computed.

As the title compound is monobasic acid, it undergoes ionization prior to its binding with metal ion. As the understanding of donor acceptor properties is prerequisite to establish binding modes, in the present investigation the geometry optimization is also carried out with ionized form of Cl-PTMP. Further the eigen values and orbital contour maps for HOMO and LUMO of ionized form were deduced.

The comparison of  $E_{\text{HOMO}}$  and  $E_{\text{LUMO}}$  in neutral and ionized form reveals better donor properties of latter form as its corresponding binding energy value of electrons in HOMO is low. As well as the energy gap between HOMO and LUMO being less in ionized form, it infers more reactivity towards binding with metal ions.

## 3.3. Equilibrium Studies on Cl-PTMP

The proton-ligand dissociation constant was determined in 70% dioxane-water mixture at 303 K and 0.1 M

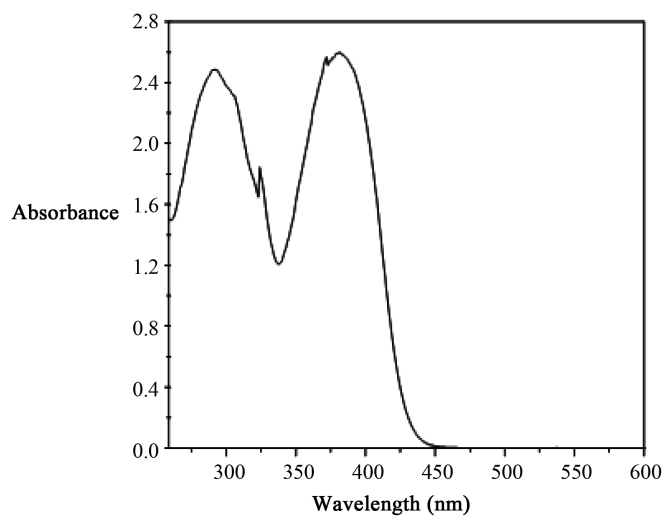


**Figure 4.** UV spectrum of Cl-PTMP.

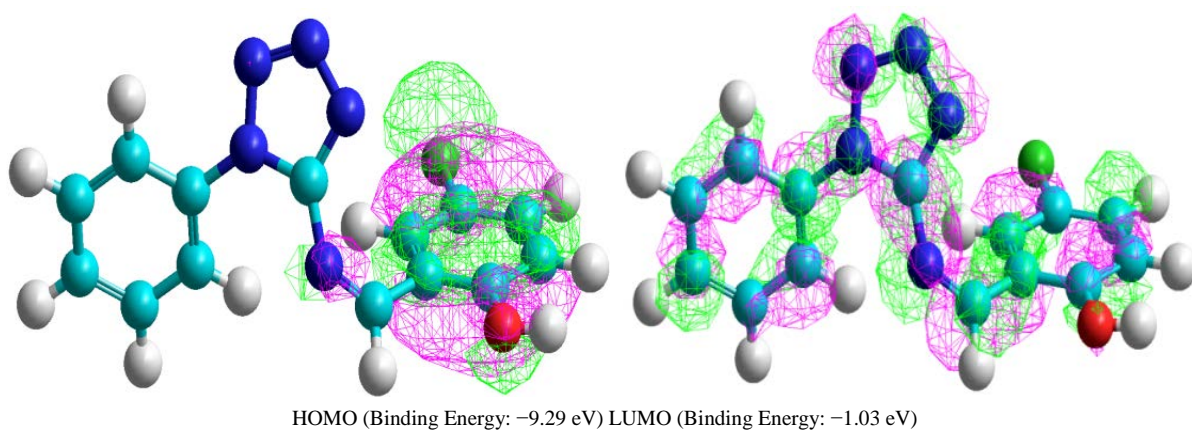


**Figure 5.** The contour maps of highest occupied molecular orbitals and lowest unoccupied molecular orbitals of Cl-PTMP neutral form.

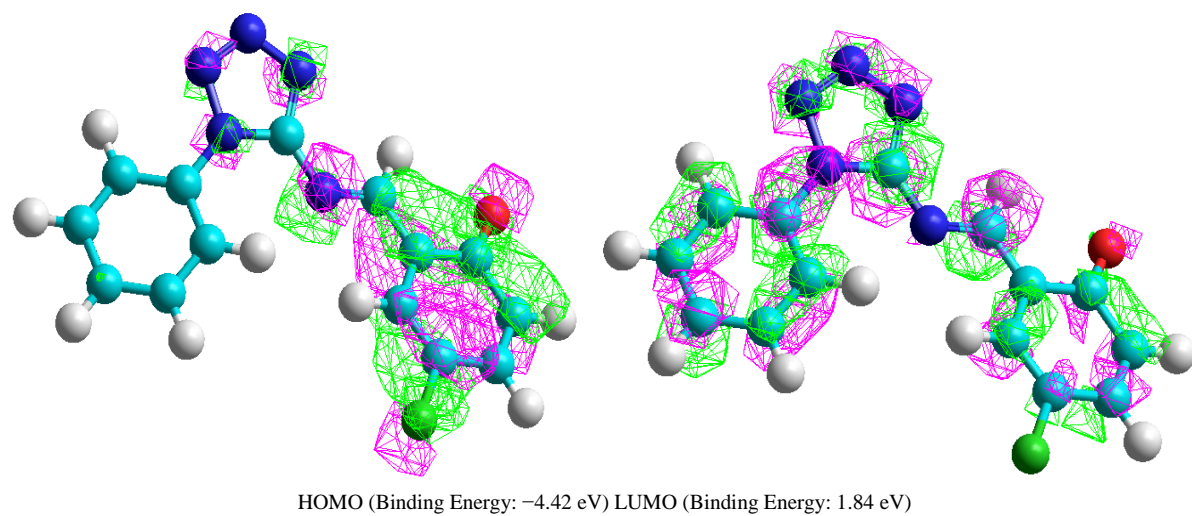


**Figure 6.** The contour maps of highest occupied molecular orbitals and lowest unoccupied molecular orbitals of ionized form of Cl-PTMP.

(KNO<sub>3</sub>) ionic strength. The  $\bar{n}_A$  values were calculated by the Irving-Rossotti method [13]-[20] and the pK<sub>a</sub> value is calculated by using linear plot method (Figure 7). The results of linear plot method revealed presence of one dissociable proton from phenolic OH with pK<sub>a</sub> value of 9.32. The pH curves of Cu-Ligand and Co-Ligand also indicate complex formation by release of proton in presence of metalions (Figure 8).

### 3.4. Spectrophotometric Studies on Cl-PTMP

Spectrophotometric study was performed by Job's continuous-variation method. The solutions of Cu (II) and Cl-PTMP with same molar concentration (0.001 M) were mixed by varying the volume but keeping the total volume constant. The pH of solution was maintained by adding 2.5 ml of buffer solution (sodium acetate + acetic acid in 3:1 ratio). The absorbance for each solution was measured at  $\lambda_{\text{max}} = 417$  nm. The curve was plotted as a function of mole fraction of ligand versus absorbance. The results revealed the stoichiometry of metal complex as 1:2 (ML<sub>2</sub>) (Figure 9).

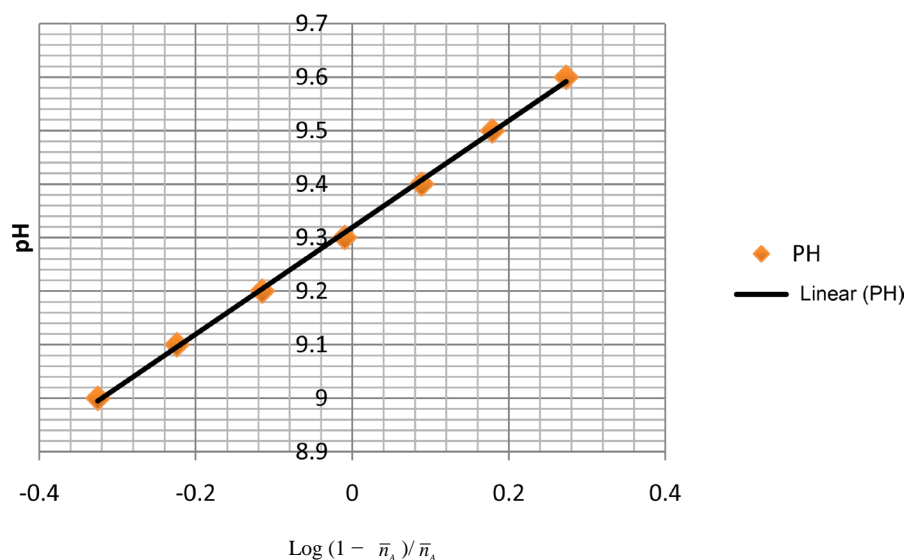


Figure 7. Plot of  $\log (1 - \bar{n}_A) / \bar{n}_A$  vs pH of Cl-PTMP in 70% v/v Dioxane-water Medium.

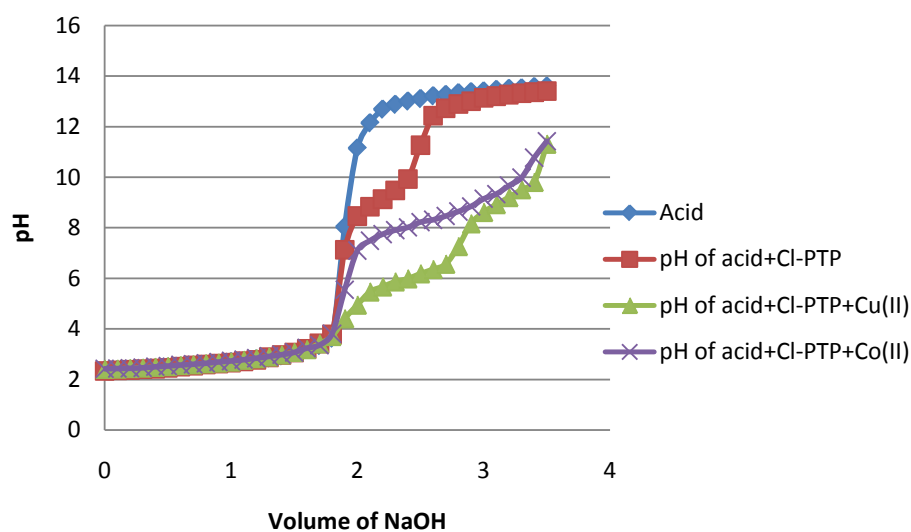
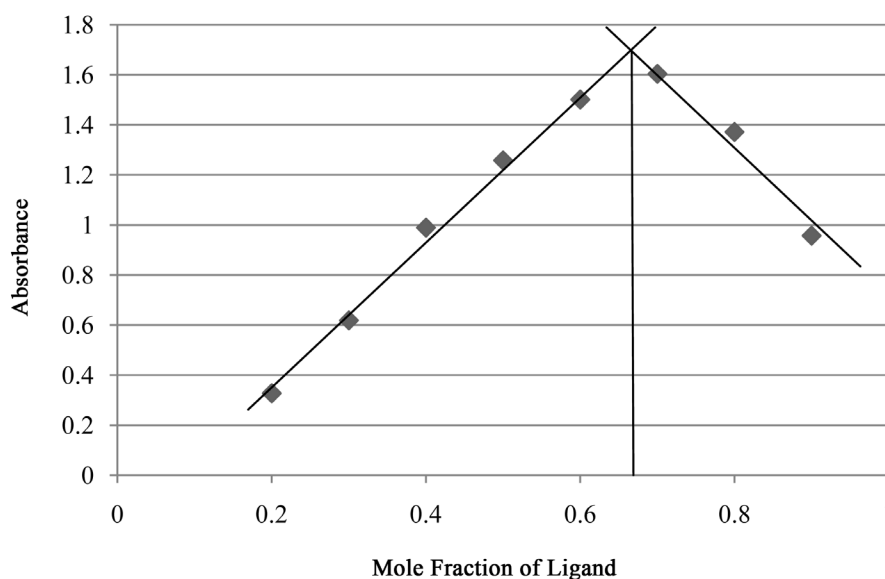


Figure 8. pH titration curves of Cl-PTMP and its Cu (II), Co (II) binary system in 70% v/v Dioxan-water medium at 303 K and 0.1 M ionic strength.



**Figure 9.** Plot of absorbance vs mole fraction of ligand.

### 3.5. Characterization of Copper and Cobalt Complexes of Cl-PTMP

#### 3.5.1. IR Spectral Data

The comparison of IR stretching frequency between Cl-PTMP and its metal complexes are presented in (Table 1) which reveals the structural changes in former upon coordination. The stretching frequency of azomethine group ( $\text{N}=\text{CH}^-$ ) in Cl-PTMP is observed at  $1605\text{ cm}^{-1}$ , while in Cu (II) and Co (II) Cl-PTMP complexes the observed higher frequencies at  $1620\text{ cm}^{-1}$  and  $1626\text{ cm}^{-1}$  respectively indicates antibonding character of highest occupied molecular orbitals (HOMO) from which electron pair is donated and thus inferring participation of ( $\text{N}=\text{CH}^-$ ) nitrogen in M-N bond formation. The new bands due to Cu-O and Co-O appear at  $569\text{ cm}^{-1}$  and  $516\text{ cm}^{-1}$  respectively. On the other hand, peaks at  $446\text{ cm}^{-1}$  and  $455\text{ cm}^{-1}$  are attributed to Cu-N and Co-N stretching vibrations respectively. The peaks in the range of  $3200 - 3400\text{ cm}^{-1}$  are due to presence of coordinated water molecules in complexes (Figure 10 and Figure 11) which can also be ascertained from TGA studies.

#### 3.5.2. Electronic Spectral Data

The UV-Visible spectra of Cu (II) and Co (II) complexes were recorded in DMSO. In Cu (II)-Cl-PTMP complex (Figure 12), the bands at  $34,965.03\text{ cm}^{-1}$  and  $26,881.72\text{ cm}^{-1}$  are observed. While for Co (II) complex (Figure 13), band appears at  $38,461.54\text{ cm}^{-1}$  which is due to charge transfer transition. The absorption band at  $24,752.48\text{ cm}^{-1}$  is attributed to d-d transition.

#### 3.5.3. Mass Spectrum of Cu (II)-Cl-PTMP

The mass spectrum (Figure 14) exhibited peak at  $m/z$  702 which corresponds to the mass of Cu (II)-Cl-PTMP complex.

#### 3.5.4. Mass Spectrum of Co (II)-Cl-PTMP

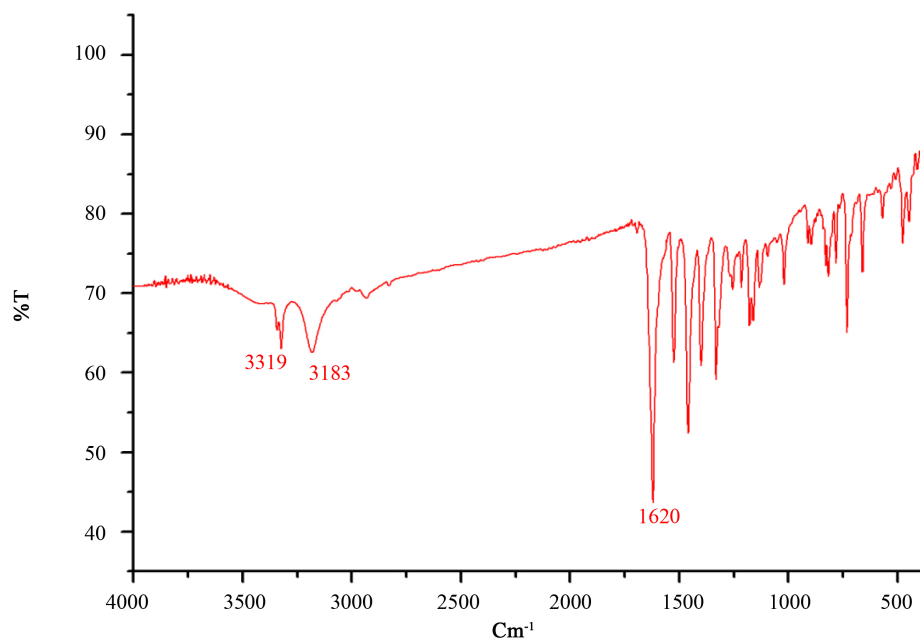
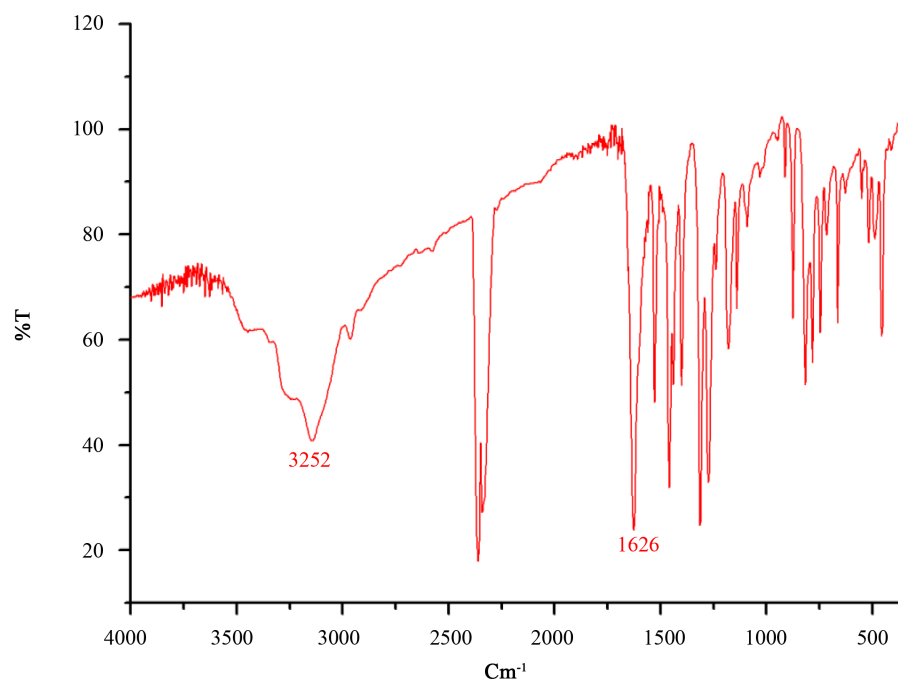
The peak recorded at  $m/z = 695$  in the mass spectrum of Co (II)-Cl-PTMP complex (Figure 15) corresponds to 1:2 metal-ligand composition.

### 3.6. Thermo-Analytical Studies

TGA data of the Cu (II)-Cl-PTMP complex displays 2 stages of weight loss. The first weight loss at  $180^\circ\text{C}$  corresponds to the loss of coordinated water and is accompanied by an endothermic trough in DTA at  $t_{\min} = 180^\circ\text{C}$ . Second weight loss around  $270^\circ\text{C}$  to  $380^\circ\text{C}$  is due to decomposition of ligand moiety with the release of heat which is evident from appearance of exothermic peak in DTA curve at  $t_{\min} = 202^\circ\text{C}$ . This exothermic peak may be due to explosive or pyrolytic nature of tetrazoleimine base moiety. The final residue is found to be 14.1%

**Table 1.** Comparison of IR stretching frequencies in Cl-PTMP and its complexes.

S. No	Compound	$\nu_{\text{CH=N}}$	$\nu_{\text{M-N}}$	$\nu_{\text{M-O}}$	$\nu_{\text{OH/H}_2\text{O}}$
1	Cl-PTMP	1605 $\text{cm}^{-1}$	-	-	-
2	Cu(II)Cl-PTMP	1620 $\text{cm}^{-1}$	446 $\text{cm}^{-1}$	569 $\text{cm}^{-1}$	3323 $\text{cm}^{-1}$
3	Co(II)Cl-PTMP	1626 $\text{cm}^{-1}$	455 $\text{cm}^{-1}$	516 $\text{cm}^{-1}$	3233 $\text{cm}^{-1}$

**Figure 10.** IR Spectrum of Cu (II) complex.**Figure 11.** IR Spectrum of Co (II) complex.



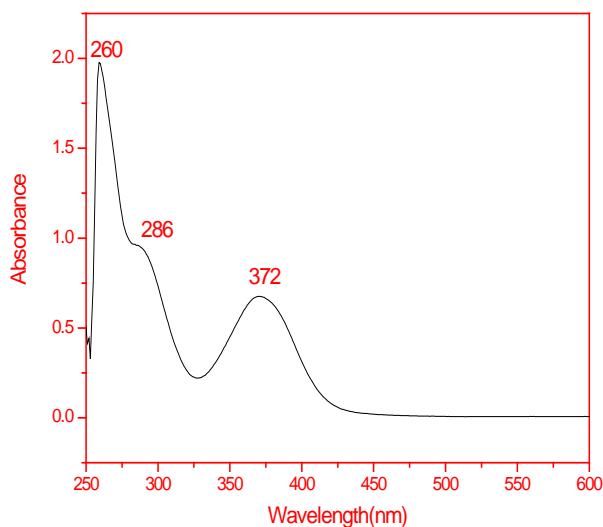


Figure 12. Electronic spectra of Cu (II) complex.

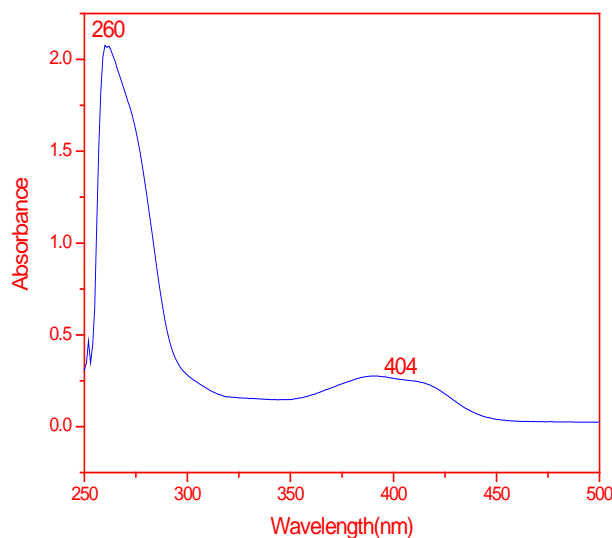


Figure 13. Electronic spectra of Co (II) complex.

which is in accordance with expected metal oxide residue (**Figure 16** and **Figure 17**).

TGA of Co (II)-Cl-PTMP complex exhibits 4 stages of weight loss. First stage of weight loss is observed at 240°C where the DTA curve also shows trough (endothermic peak) corresponding to the loss of coordinated water molecule. At 450°C partial decomposition of ligand takes place which is accompanied by an exothermic peak on DTA. Further decomposition above 630°C observed is attributable to total loss of organic moiety in complex. The residual mass of 24.7% at 1000°C probably corresponds to metal oxide moiety (**Figure 18** and **Figure 19**).

### 3.7. SEM and EDX of Cl-PTMP and Its Complexes

Scanning Electron Microscope (SEM) was used to investigate the morphology of Cl-PTP, its Cu (II) and Co (II) complexes. SEM image of Cl-PTMP in the resolution of 400  $\mu\text{m}$  is viewed as needle type particles. There is conspicuous change in themorphology of title compound when coordinated with a metal ion. In Cu (II) and Co (II) complexes the characteristic morphologies were observed with the image resolution of 200  $\mu\text{m}$  and 80  $\mu\text{m}$  respectively. The elemental composition of Cl-PTMP and its Cu (II), Co (II) complexes were identified with

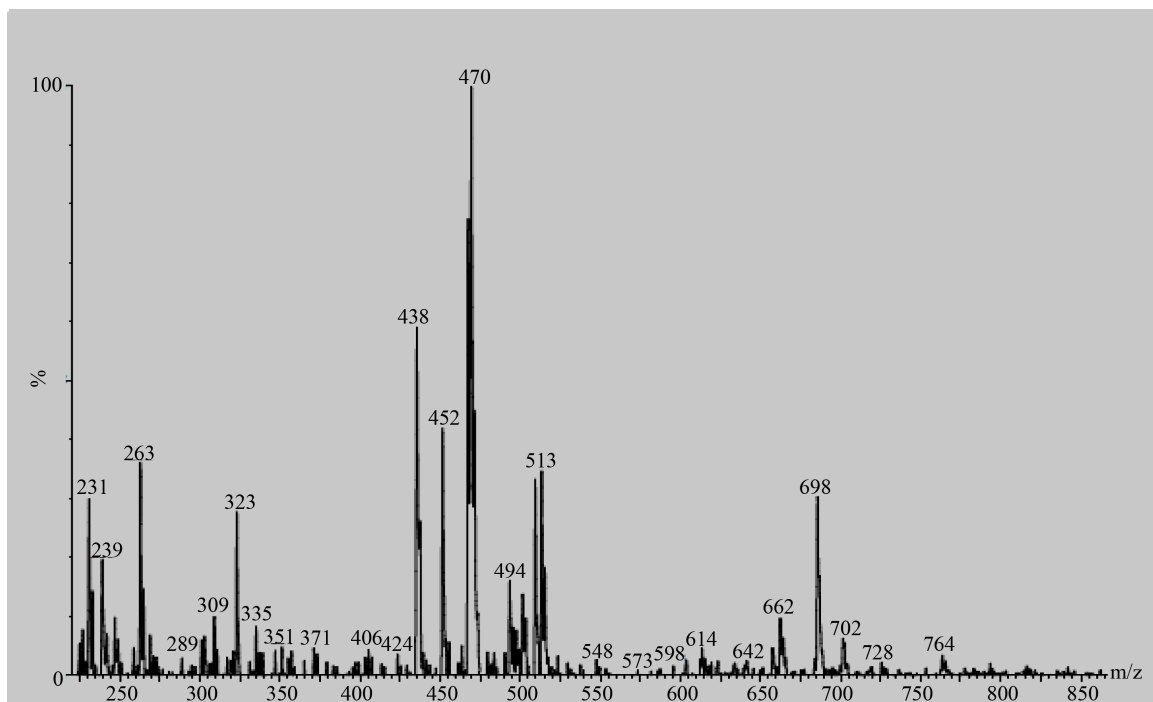


**Figure 14.** Mass spectrum of Cu (II)-Cl-PTMP.

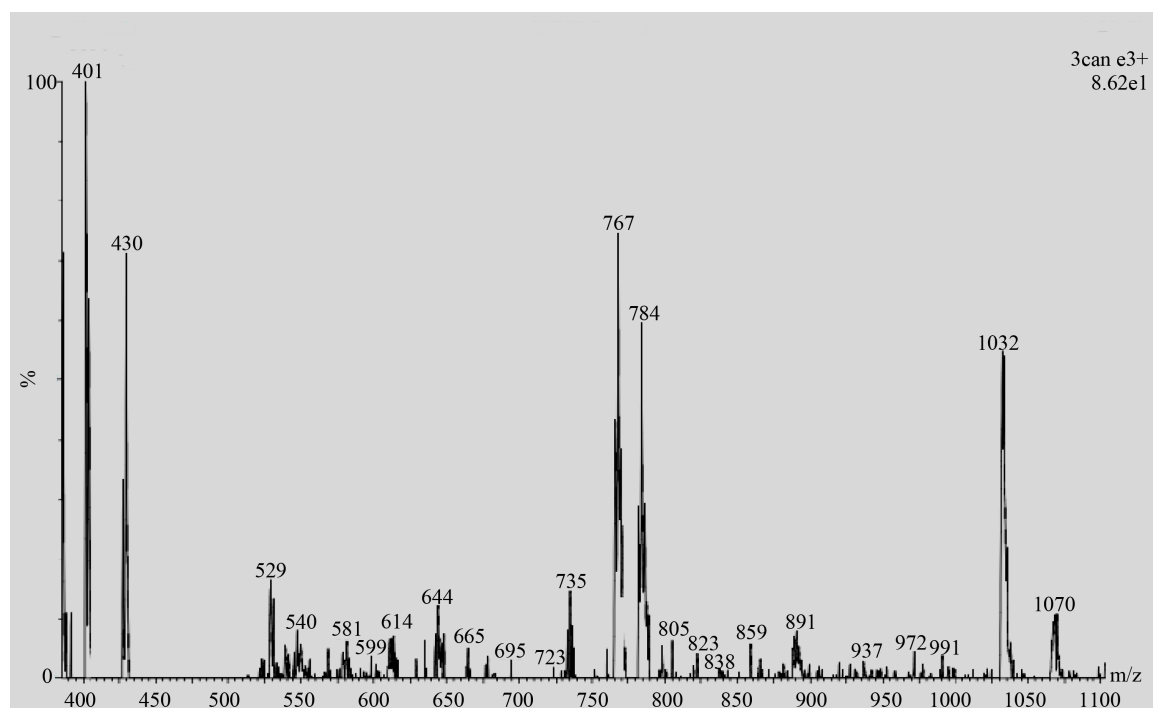


**Figure 15.** Mass spectrum of Co (II)-Cl-PTMP.

EDX analysis (**Figures 20-22**).

### 3.8. Biological Studies

The newly synthesized tetrazole derivative Cl-PTMP and its metal complexes were investigated for their inhibition

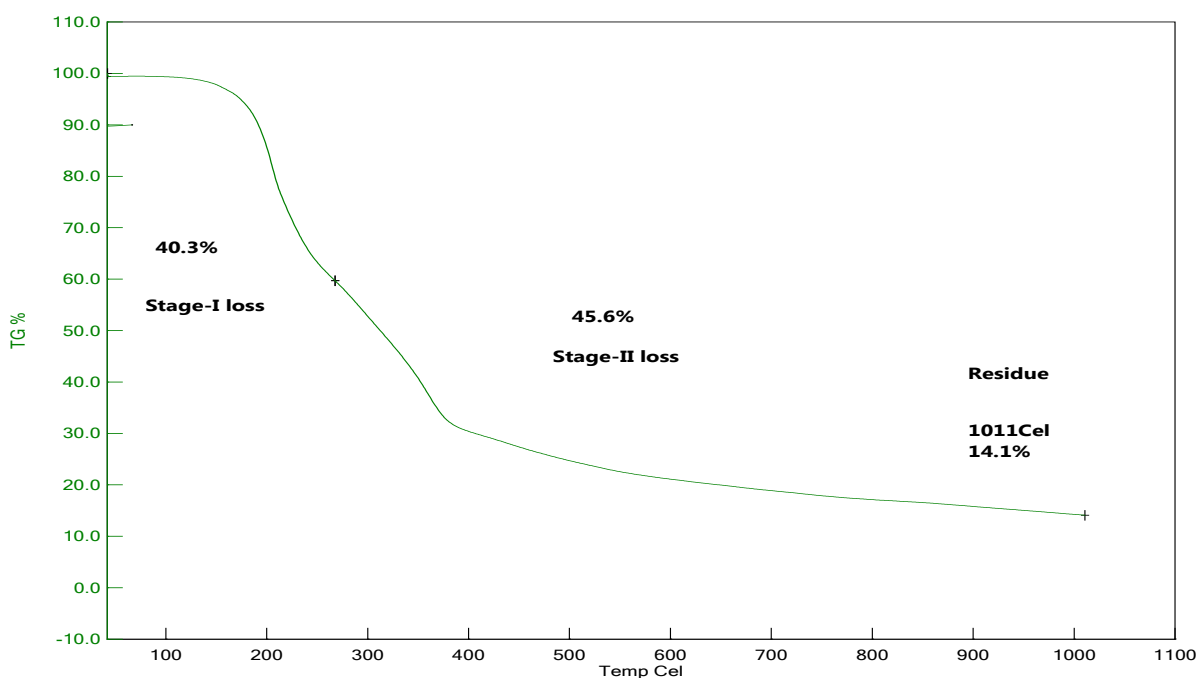


Figure 16. TGA curve of Cu (II)-Cl-PTMP.

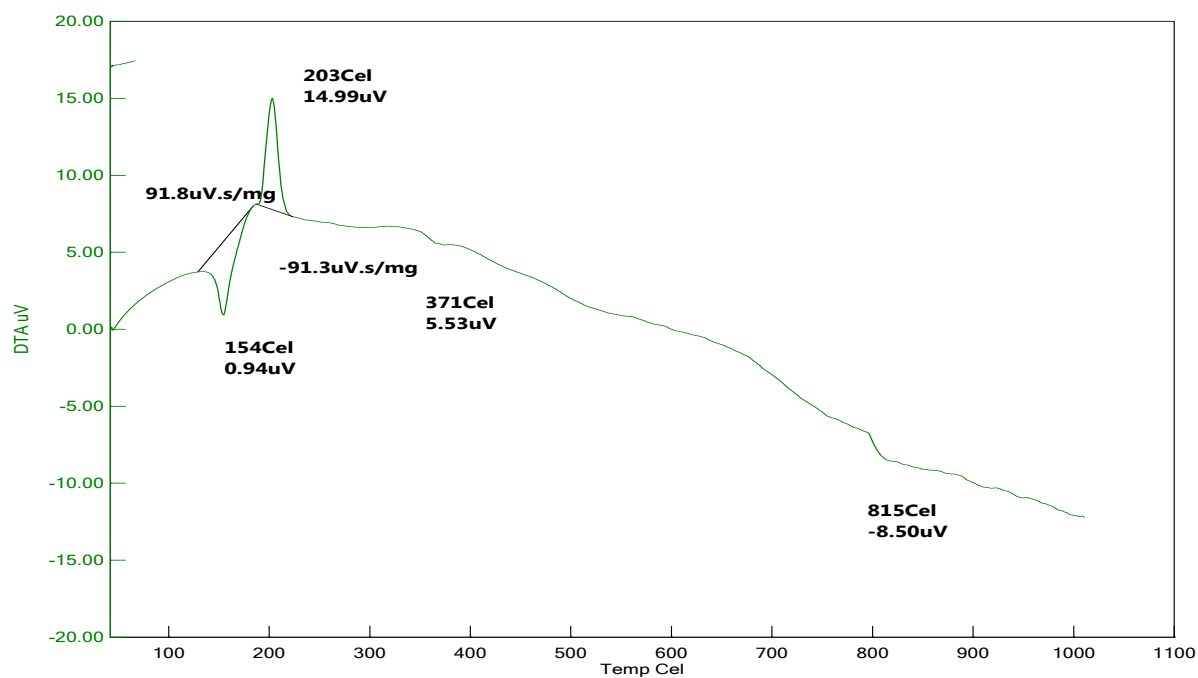
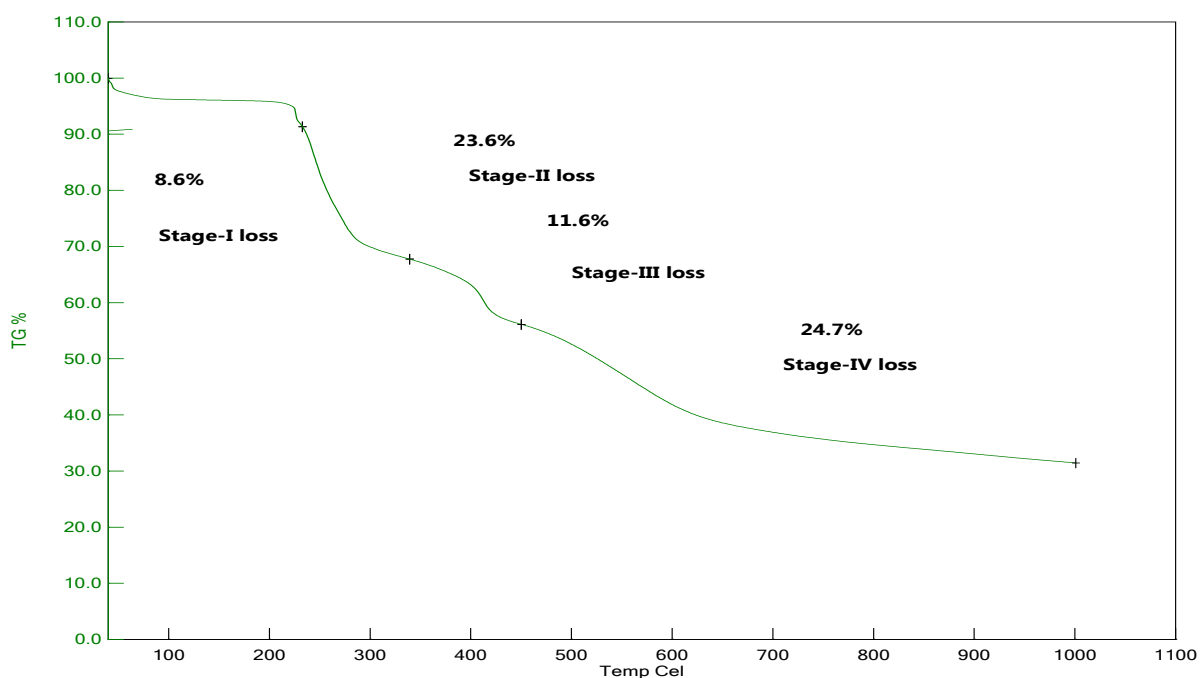
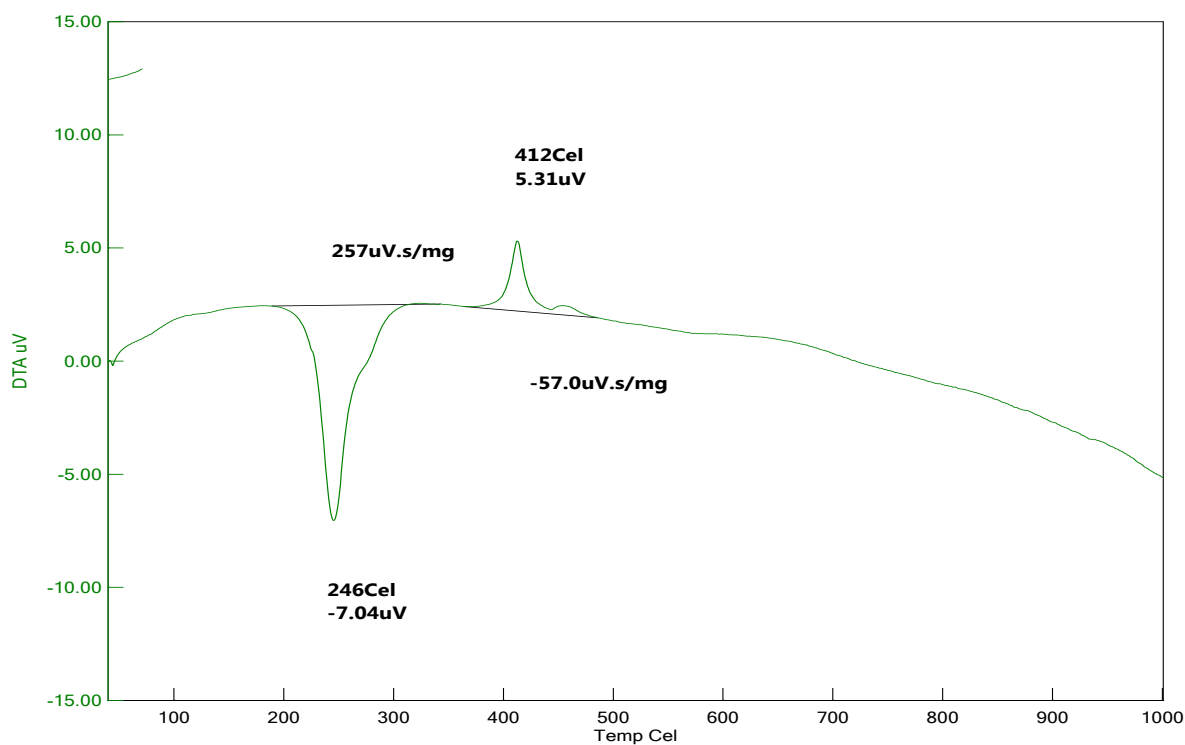


Figure 17. DTA curve of Cu (II)-Cl-PTMP.

growth against Gram positive (*Staphylococcus aureus* and *Bacillus*), Gram negative (*Escherichia coli*, *Pseudomonas* and *Klebsiella*) bacteria and yeast (*Yepda*) strains by the discdiffusion method. The organism was spread on nutrient agar (1% beef extract, 1% peptone, 0.5 NaCl and 1.5 agar agar) and then 20  $\mu$ l each of Cl-PTMP, Cu (II) and Co (II) complexes with concentration of 1 mg/1ml were inoculated into the wells created on agar plates by using sterile 6 mm diameter well borer. Then the respective petri dishes were kept in refrigerator for 15 minutes and subsequently allowed for incubation process at 30°C/48 hours for yeast and 37°C/24 hours for



**Figure 18.** TGA curve of Co (II)-Cl-PTMP.



**Figure 19.** DTA curve of Co (II)-Cl-PTMP.

bacteria. The antimicrobial activity was determined by measuring the diameter of the inhibition zone (in mm scale) ([Table 2](#)).

Antimicrobial activity studies revealed that free Cl-PTMP is less active than its coordinated form with metal ions Cu (II) and Co (II), wherein Co-Cl-PTMP exhibited more enhanced activity.

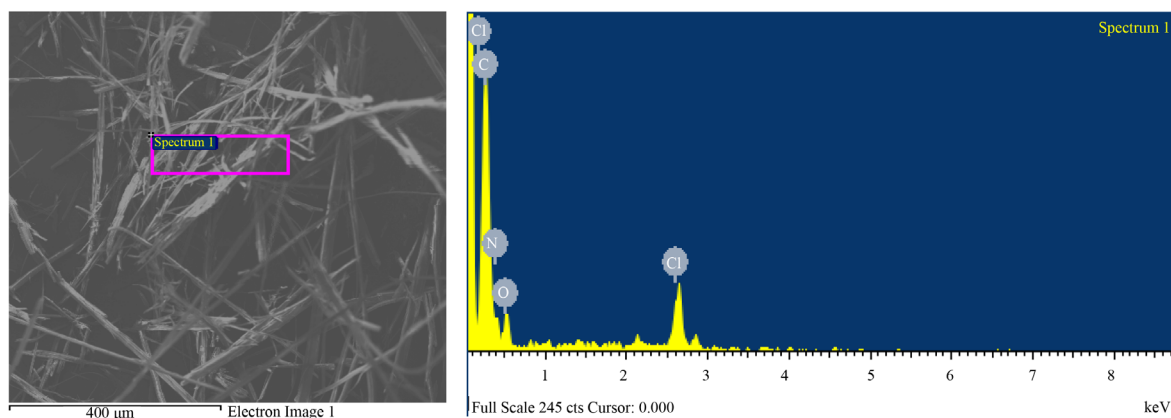


**Figure 20.** SEM Image and EDX spectrum of Cl-PTMP.

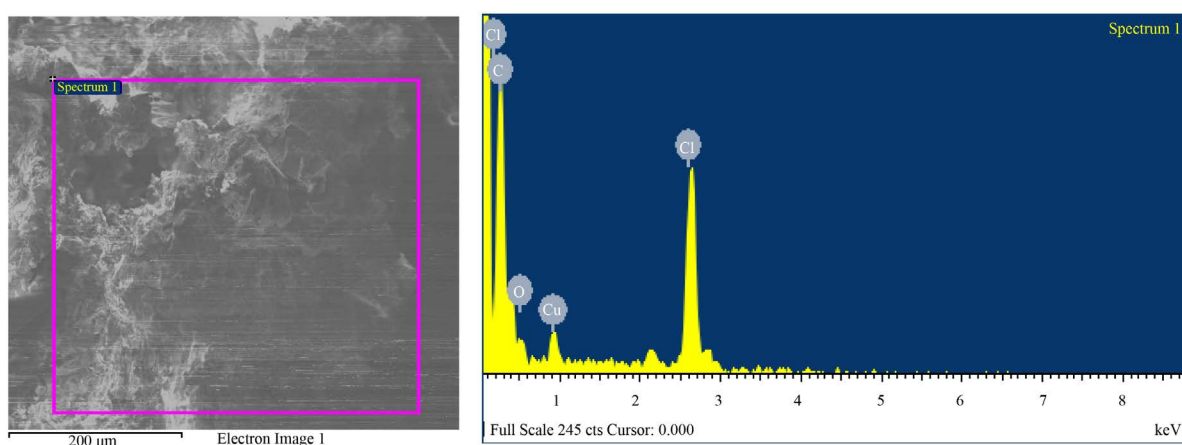


**Figure 21.** SEM Image and EDX spectrum of Cu (II)-Cl-PTMP.

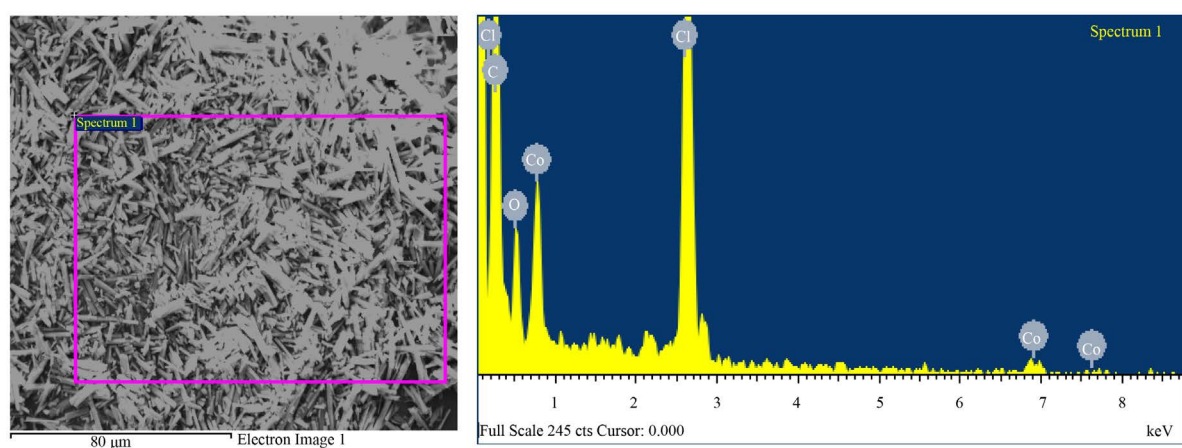


**Figure 22.** SEM Image and EDX spectrum of Co (II)-Cl-PTMP.

#### 4. Conclusion

The new imine base Cl-PTMP and its Cu (II) and Co (II) complexes were synthesized and characterized by the data obtained from various spectro-analytical techniques. Mass spectrum of Cl-PTMP revealed appearance of  $M + 1$  peak and its elemental composition was ascertained from EDX data. Further IR,  $^1\text{H-NMR}$  and UV-Vis spectral data are further informative to establish its structural properties. The eigen values for molecular orbitals

**Table 2.** Antimicrobial activity of Cl-PTMP and its Cu (II), Co (II) complexes.

Bacteria	Cl-PTMP	Cu-Cl-PTMP	Co-Cl-PTMP
<i>Bacillus subtilis</i>	2 mm	3 mm	4 mm
<i>E. coli</i>	2 mm	3 mm	5 mm
<i>Pseudomonas</i>	2 mm	3 mm	4 mm
<i>Klebsiella</i>	2 mm	3 mm	4 mm
<i>Staphylococcus</i>	2 mm	5 mm	5 mm
Yepda	1 mm	4 mm	4 mm

and the energy gap between HOMO and LUMO were computed for the geometry optimized molecule of Cl-PTMP in both neutral and ionized forms using hyperchem 7.5 tools. The comparison of results revealed that the binding energy of HOMO electrons and the gap between HOMO and LUMO in ionized form was less and thus inferring more reactivity of ionized form towards metal ion coordination. pH metry and spectrophotometry results revealed the stoichiometry of metal complex as 1:2 (ML<sub>2</sub>). This new imine base and its complexes were investigated for the antimicrobial activity. The antimicrobial activity follows the order: Co (II)-Cl-PTMP > Cu (II)-Cl-PTMP > Cl-PTMP indicating more pronounced activity in complexes rather than in free uncoordinated Cl-PTMP.

## Acknowledgements

The authors thank the staff of the Instrumentation Lab, Department of Chemistry and Department of Central Facilities for Research & Development (CFRD), Osmania University and Hyderabad for recording UV-Vis, IR and <sup>1</sup>H-NMR spectra. We are also thankful to Department of Microbiology, Osmania University for providing necessary facilities.

## References

- [1] Myznikov, L.V., Hrabalek, A. and Koldobskii, G.I. (2007) Drugs in the Tetrazole Series. (Review). *Chemistry of Heterocyclic Compounds*, **43**, 1-9. <http://dx.doi.org/10.1007/s10593-007-0001-5>
- [2] Schocken, M.J., Creekmore, R.W., Theodoridis, G., Nystrom, G.J. and Robinson, R.A. (1989) Microbial Transformation of the Tetrazolinone Herbicide f5231. *Applied and Environmental Microbiology*, **55**, 1220.
- [3] Butter, R.N., Katritzky, A.R. and Rees, C.W. (1984) The Structure, Reactions, Synthesis and Uses of Heterocyclic Compounds. *Comprehensive Heterocyclic Chemistry*, **5**, 791.
- [4] Mavromoustakos, T., Kolocouris, A., Zervou, M., Roumelioti, P., Matsoukas, J. and Weisemann, R. (1999) An Effort to Understand the Molecular Basis of Hypertension through the Study of Conformational Analysis of Losartan and Sarmesin Using a Combination of Nuclear Magnetic Resonance Spectroscopy and Theoretical Calculations. *Journal of Medicinal Chemistry*, **42**, 1714-1722. <http://dx.doi.org/10.1021/jm980499w>
- [5] Mekni, N. and Bakloiti, A. (2008) Synthesis of New 1-Substituted 4-Perfluoroalkyl Tetrazol-5-Ones. *Journal of Fluorine Chemistry*, **129**, 1073-1075. <http://dx.doi.org/10.1016/j.jfluchem.2008.06.019>
- [6] Burger, A. (1991) Isosterism and Bioisosterism in Drug Design. *Progress in Drug Research*, **37**, 287.
- [7] Ranjithreddy, P., Jaheer, M., Narsimha, N., Srinivas, B. and Sarala Devi, Ch. (2014) Synthesis, Characterization, Biological Activity and DNA Cleavage Studies on Tetrazole Imine Base and Their Metal Complexes—An Experimental and Theoretical Approach. *IOSR Journal of Pharmacy*, **4**, 21.
- [8] Broo, A. and Lincoln, P. (1997) *Ab Initio* and Semiempirical Calculations of Geometry and Electronic Spectra of Ruthenium Organic Complexes and Modeling of Spectroscopic Changes upon DNA Binding. *Inorganic Chemistry*, **36**, 2544-2553. <http://dx.doi.org/10.1021/ic961193n>
- [9] Gilpin, R.K. and Predicting, I.D. (1995) Predicting 1D NMR Spectra. *Analytical Chemistry*, **67**, 541. <http://dx.doi.org/10.1021/ac00113a722>
- [10] Vanciuc, O. (1996) HyperChem Release 4.5 for Windows. *Journal of Chemical Information and Computer Sciences*, **36**, 612. <http://dx.doi.org/10.1021/ci950190a>
- [11] Winchester, W.R. and Doyle, M.P. (1992) Computer Software Reviews. *Journal of the American Chemical Society*, **114**, 9243. <http://dx.doi.org/10.1021/ja00049a600>

- [12] Witanowski, W., Biedrzycka, Z., Sicinska, W., Grabowski, Z. and Webb, G.A. (1996) Solvent Effects on the Nitrogen NMR Shieldings in Oxazole and Oxadiazole Systems. *Journal of Magnetic Resonance, Series A*, **120**, 148-154. <http://dx.doi.org/10.1006/jmra.1996.0112>
- [13] Irving, H.M. and Rossotti, H.S. (1954) The Calculation of Formation Curves of Metal Complexes from pH Titration Curves in Mixed Solvents. *Journal of Chemical Society (Resumed)*, 2904-2910. <http://dx.doi.org/10.1039/jr9540002904>
- [14] Irving, H.M. and Rossetti, H.S. (1953) 680. Methods for Computing Successive Stability Constants from Experimental Formation Curves. *Journal of Chemical Society (Resumed)*, 3397-3405. <http://dx.doi.org/10.1039/jr9530003397>
- [15] Irving, H.M. and Rossotti, H.S. (1956) Some Relationships among the Stabilities of Metal Complexes. *Acta Chemica Scandinavica*, **10**, 72-93. <http://dx.doi.org/10.3891/acta.chem.scand.10-0072>
- [16] Laxmi, K., Bhargavi, G., Sireesha, B. and Sarala Devi, C. (2006) Interaction of 2-(2'-Hydroxy)Phenylbenzothiazoline with Some Metal Ions: Determination of Its Dissociation Constant in Aquo-Organic Media. *Bulletin of the Chemical Society of Ethiopia*, **20**, 161-166. <http://dx.doi.org/10.4314/bcse.v20i1.21156>
- [17] Bhargavi, G., Sireesha, B. and Sarala Devi, C. (2002) A Study on Coordination Properties of 3-Mercapto-1,2,4-Triazole in Solution and Characterization of Its Solid Metal Complexes. *Bulletin of Pure and Applied Sciences*, **21C**, 1.
- [18] Bhargavi, G., Sireesha, B. and Sarala Devi, C. (2002) A Study on Potential Donor Sites of Some Substituted 1,2,4-Triazoles and Their Denticity. *Journal of the Indian Chemical Society*, **79**, 826.
- [19] Sireesha, B., Bhargavi, G., Sita, C. and Sarala Devi, C. (2006) Interaction of 2-(2'-Hydroxy) Phenyl Benzothiazoline with Some Metal Ions: Determination of Its Dissociation Constant in Aquo-Organic Media. *Bulletin of Pure and Applied Sciences*, **25C**, 1.
- [20] Aliya, Sireesha, B., Venkata Ramana Reddy, C. and Sarala Devi, C. (2008) Spectral and Equilibrium Studies on Some New Derivatives of 4-Amino-5-Phenyl-3-Mercapto-1,2,4-Triazole. *Journal of the Indian Chemical Society*, **85**, 926-929.